GAMOW–TELLER RESPONSE CALCULATED IN QUASIPARTICLE RANDOM PHASE APPROXIMATION PLUS QUASIPARTICLE VIBRATION COUPLING MODEL*

Yifei Niu[a], Gianluca Colò[b,c], Enrico Vigezzi[c]

[a]ELI–NP, "Horia Hulubei" National Institute
for Physics and Nuclear Engineering
30 Reactorului Street, 077125 Bucharest, Măgurele, Romania
[b]Dipartimento di Fisica, Università degli Studi di Milano
via Celoria 16, 20133 Milano, Italy
[c]INFN — Sezione di Milano, via Celoria 16, 20133 Milano, Italy

(Received January 15, 2018)

The self-consistent quasiparticle random phase approximation (QRPA) plus quasiparticle-vibration coupling (QPVC) with Skyrme interactions is used to describe the Gamow–Teller (GT) response in open-shell nuclei. The effect of superfluidity, including both the isoscalar spin-triplet and the isovector spin-singlet pairing interactions, is taken into account in both the ground state and the excited states. Zero-range pairing forces of volume-type and surface-type are both used in our investigation. The phonon properties and GT strength distributions obtained with either type of force are compared, by taking the superfluid nucleus ^{120}Sn as an example. In both cases, a spreading width is developed, and the agreement with experimental data of the strength distribution in ^{120}Sn is improved with the inclusion of QPVC effect.

DOI:10.5506/APhysPolBSupp.11.127

1. Introduction

As one of the most important spin–isospin excitation modes, the Gamow–Teller (GT) excitation not only provides useful constraints on the spin–isospin channel of nuclear effective interaction, but also plays an important role in the nuclear weak interactions processes [1, 2], such as β decay [3], electron capture [4, 5] and neutrino nucleus scattering [6, 7].

* Presented at the XXIV Nuclear Physics Workshop "Marie and Pierre Curie", Kazimierz Dolny, Poland, September 20–24, 2017.

Two kinds of microscopic approaches are widely used in the study of GT excitations, which are the shell model and the random-phase approximation (RPA) approach (or quasiparticle RPA (QRPA) for superfluid nuclei). Due to the large configuration space, accurate shell model calculations are not feasible for heavy nuclei away from magic numbers [2, 8, 9]. The QRPA approach can be applied to all nuclei in principle except for a few very light systems. The self-consistent QRPA approach based on Skyrme [10–16] or relativistic [3, 17–19] density functionals successfully reproduces the overall properties of charge-exchange excitations like the centroid energy if the energy density functional is properly calibrated.

However, the width of GT resonance cannot be described in a satisfactory way within the QRPA model. In QRPA, the GT excitation is treated as a superposition of two quasiparticle (2qp) excitations and, therefore, cannot account for the spreading width, which originates form the transfer of energy and angular momentum from the collective motion to more complicated nuclear states having 4qp, . . . , $n$qp character. More complicated configurations should be included in the model space. One way is to include the quasiparticle vibration coupling (QPVC) effect in the QRPA model, which forms the so-called QRPA+QPVC model. In the QRPA+QPVC model, the 2 quasiparticle configurations are coupled to collective vibrational phonons [20–22]. As a first step, the self-consistent RPA+particle vibration coupling (PVC) approach without pairing correlations for GT excitations was established within both the relativistic [23,24] and the non-relativistic framework [25,26]. It has been shown that a spreading width is developed with the inclusion of PVC effects, and thus a good agreement with experimental data for the GT resonance (GTR) is obtained. The RPA+PVC model has been further applied to β decay [27], and it greatly improves the β-decay half-lives in magic nuclei compared to the RPA result. The pairing correlations were then also included, and the self-consistent QRPA+QPVC model was developed based on the Skyrme or relativistic density functionals. This model has been applied for the study of GT excitations in superfluid nuclei [28,29]. In Ref. [28], the GT excitation in ^{120}Sn was studied by using a density-dependent, zero-range surface pairing force within the Skyrme density functional framework.

In this work, we will study the GT excitation in ^{120}Sn with QRPA and QRPA+QPVC models based on a Skyrme density functional using a zero-range pairing force of volume or of surface character, and we will compare the corresponding results, such as phonon properties and GT strength distributions.

2. Formulas

Firstly, a HFB calculation is performed to obtain the properties of quasiparticles. Then the charge-exchange QRPA model is used to get the GT

strength. The detailed formulas of charge-exchange QRPA on top of HFB can be found in Ref. [10]. The isovector $T = 1$ pairing is included both in the ground state and in the residual interaction used in the QRPA calculation. Moreover, the isoscalar $T = 0$ pairing is also included in the residual interaction in the QRPA calculation. The necessity of isoscalar $T = 0$ pairing has been discussed in many previous works, especially in connection with the low-lying GT strength of $N = Z + 2$ nuclei and the β-decay half-lives [3, 10, 30–34]. The pairing force we use is a zero-range pairing force parameterized as follows:

$$V_{T=1}(\boldsymbol{r}_1, \boldsymbol{r}_2) = V_0 \frac{1 - P_\sigma}{2} \left(1 - \eta \frac{\rho(\boldsymbol{r})}{\rho_0}\right) \delta(\boldsymbol{r}_1 - \boldsymbol{r}_2), \tag{1}$$

$$V_{T=0}(\boldsymbol{r}_1, \boldsymbol{r}_2) = f V_0 \frac{1 + P_\sigma}{2} \left(1 - \eta \frac{\rho(\boldsymbol{r})}{\rho_0}\right) \delta(\boldsymbol{r}_1 - \boldsymbol{r}_2), \tag{2}$$

where $\boldsymbol{r} = (\boldsymbol{r}_1 + \boldsymbol{r}_2)/2$. ρ_0 is taken to be $\rho_0 = 0.16$ fm^{-3}, and P_σ is the spin exchange operator. $\eta = 0$ or 1 represents volume or surface pairing. The pairing strength V_0 is determined in such a way that it can reproduce the experimental pairing gap for the nucleus to be studied, like ^{120}Sn in this paper. In the $T = 0$ channel, the pairing strength cannot be constrained from the ground-state calculation as in the $T = 1$ channel, however, several different types of analysis suggest the value of proportionality factor f to be close to 1, or slightly larger [35]. Accordingly, in this work we adopt $f = 1$.

The QRPA+QPVC equation reads

$$\begin{pmatrix} \mathcal{D} + \mathcal{A}_1(E) & \mathcal{A}_2(E) \\ -\mathcal{A}_3(E) & -\mathcal{D} - \mathcal{A}_4(E) \end{pmatrix} \begin{pmatrix} F^{(\nu)} \\ \bar{F}^{(\nu)} \end{pmatrix} = \left(\Omega_\nu - i\frac{\Gamma_\nu}{2}\right) \begin{pmatrix} F^{(\nu)} \\ \bar{F}^{(\nu)} \end{pmatrix}. \tag{3}$$

$\mathcal{D}$ is a diagonal matrix containing the physical QRPA eigenvalues. The $\mathcal{A}_i$ matrices are complex and energy-dependent, associated with the coupling to the doorway states. The expressions of $\mathcal{A}_i$ in the QRPA basis $|n\rangle$ are given by

$$(\mathcal{A}_1)_{mn} = \sum_{ab,a'b'} W^{\downarrow}_{ab,a'b'}(E) X^{(m)}_{ab} X^{(n)}_{a'b'} + W^{\downarrow *}_{ab,a'b'}(-E) Y^{(m)}_{ab} Y^{(n)}_{a'b'}, \tag{4}$$

$$(\mathcal{A}_2)_{mn} = \sum_{ab,a'b'} W^{\downarrow}_{ab,a'b'}(E) X^{(m)}_{ab} Y^{(n)}_{a'b'} + W^{\downarrow *}_{ab,a'b'}(-E) Y^{(m)}_{ab} X^{(n)}_{a'b'}, \tag{5}$$

$$(\mathcal{A}_3)_{mn} = \sum_{ab,a'b'} W^{\downarrow}_{ab,a'b'}(E) Y^{(m)}_{ab} X^{(n)}_{a'b'} + W^{\downarrow *}_{ph,p'h'}(-E) X^{(m)}_{ab} Y^{(n)}_{a'b'}, \tag{6}$$

$$(\mathcal{A}_4)_{mn} = \sum_{ab,a'b'} W^{\downarrow}_{ab,a'b'}(E) Y^{(m)}_{ab} Y^{(n)}_{a'b'} + W^{\downarrow *}_{ab,a'b'}(-E) X^{(m)}_{ab} X^{(n)}_{a'b'}. \tag{7}$$

$X^{(n)}_{ab}$ and $Y^{(n)}_{ab}$ are the forward-going and backward-going amplitudes associated with the QRPA eigenstates $|n\rangle$, respectively. Here and in what follows, the indices a, b label the so-called BCS quasiparticle states in the canonical basis that are those defined by the operators α and $\alpha^\dagger$ at p. 248 of Ref. [36]. Note that the T_- and T_+ channels are coupled in the QRPA and QRPA+QPVC matrices, when both protons and neutrons are superfluid, at variance with the case of RPA and RPA+PVC (and with the case in which only one of the two species is superfluid, as in ^{120}Sn). The matrix $\begin{pmatrix} \mathcal{D}+\mathcal{A}_1(E) & \mathcal{A}_2(E) \\ \mathcal{A}_3(E) & \mathcal{D}+\mathcal{A}_4(E) \end{pmatrix}$ is still symmetric as in the RPA+PVC case.

The spreading matrix $W^{\downarrow}_{ab,a'b'}(E)$ is the most important quantity in the QRPA+QPVC model,

$$W^{\downarrow}_{ab,a'b'} = \langle ab|V\frac{1}{E-\hat{H}}V\left|a'b'\right\rangle = \sum_{NN'}\langle ab|V|N\rangle\langle N|\frac{1}{E-\hat{H}}\left|N'\right\rangle\left\langle N'\right|V\left|a'b'\right\rangle\,, \tag{8}$$

where $|N\rangle = |a''b''\rangle \otimes |nL\rangle$ represents a doorway state and a'', b'' are BCS quasiparticle states, as recalled above. The doorway states are made of a two-BCS-quasiparticle excitation $|ab\rangle$ coupled to a collective vibration $|nL\rangle$ of angular momentum L and energy ω_{nL}. The properties of these collective vibrations, *i.e.*, phonons $|nL\rangle$, are obtained by computing the QRPA response with the same Skyrme interaction, for states of natural parity $L^\pi = 0^+,\ 1^-,\ 2^+,\ 3^-,\ 4^+,\ 5^-$, and 6^+. We have retained the phonons with energy less than 20 MeV and absorbing a fraction of the non-energy weighted isoscalar or isovector sum rule (NEWSR) strength larger than 5%.

The final expression for spreading matrix in angular momentum coupled form $W^{\downarrow J}_{ab,a'b'}$ reads

$$\begin{aligned}
W^{\downarrow J}_{1ab,a'b'} &= \delta_{bb'}\delta_{j_a j_{a'}}\frac{1}{\hat{j}_a^2}\sum_{a'',nL}\frac{\langle a||V||a'',nL\rangle\langle a'||V||a'',nL\rangle}{E-[\omega_{nL}+E_{a''}+E_b\pm(\lambda_n-\lambda_p)]+i\Delta}\,,\\
W^{\downarrow J}_{2ab,a'b'} &= \delta_{aa'}\delta_{j_b j_{b'}}\frac{1}{\hat{j}_b^2}\sum_{b'',nL}\frac{\langle b||V||b'',nL\rangle\langle b'||V||b'',nL\rangle}{E-[\omega_{nL}+E_{b''}+E_a\pm(\lambda_n-\lambda_p)]+i\Delta}\,,\\
W^{\downarrow J}_{3ab,a'b'} &= (-)^{j_a+j_b+J}\begin{Bmatrix} j_a & j_b & J \\ j_{b'} & j_{a'} & L \end{Bmatrix}\\
&\quad\times\sum_{nL}\frac{\langle a'||V||a,nL\rangle\langle b||V||b',nL\rangle}{E-[\omega_{nL}+E_a+E_{b'}\pm(\lambda_n-\lambda_p)]+i\Delta}\,,
\end{aligned}$$

$$W^{\downarrow J}_{4ab,a'b'} = (-)^{j_{a'}+j_{b'}+J} \left\{ \begin{array}{ccc} j_{a'} & j_{b'} & J \\ j_b & j_a & L \end{array} \right\} \times \sum_{nL} \frac{\langle a||V||a', nL\rangle\langle b'||V||b, nL\rangle}{E - [\omega_{nL} + E_{a'} + E_b \pm (\lambda_n - \lambda_p)] + i\Delta} \,. \tag{9}$$

In the above formulas, we use the identity matrix instead of the C transformation matrix which transforms HFB quasiparticles to BCS quasiparticles [28]. This represents a good approximation for nuclei not far from the stability line, like the nucleus ^{120}Sn studied in this work. $\hat{j}_i^2$ is a shorthand notation for $2j_i + 1$. E_a is the BCS quasiparticle energy. The chemical potential difference $\lambda_n - \lambda_p$ is included in the energy denominator so that it can reproduce the RPA+PVC limit for magic nuclei, where the sign '+' is for T_- excitations and '−' for T_+ excitations. The smearing parameter Δ is introduced to avoid singularities in the denominator, and a convenient practical value is $\Delta = 200$ keV. The detailed formulas can be found in Ref. [28].

The subtraction method, to avoid the double counting problem in the QPVC calculation [37–41], is used in the QPVC calculation.

3. Results and discussions

We use the Skyrme interaction SGII [42]. This will be useful, in order to assess the dependence of the results on the particular effective interaction which has been adopted, by comparing them with previous studies carried out with the SkM* interaction [28]. In the HFB calculation, we use a quasiparticle energy cutoff of 200 MeV and a maximum angular momentum $j_{\max} = 15/2$. The HFB equation is solved in coordinate space with a box radius of 20 fm. We use both the volume pairing and surface pairing, and the pairing strength is adjusted to reproduce the value of average neutron pairing gap $\Delta_n = 1.34$ MeV in ^{120}Sn derived from the empirical odd–even mass difference.

In Table I, the properties of phonons with different multipolarities calculated by QRPA model with surface and volume pairing are shown. Although the same neutron paring gap is obtained, the surface and volume pairing give different energies and transition probabilities. The volume pairing gives a smaller phonon energy which is closer to experimental data for the quadrupole case, but also a smaller transition probability for which the agreement with experimental data is worse, compared to the surface pairing case.

TABLE I

The energy and reduced transition probability of the lowest phonons of different multipolarities included in the QRPA+QPVC calculation for ^{120}Sn. The experimental data are taken from NNDC [43]. The theoretical results are obtained by the QRPA approach with the interactions SGII with surface pairing and volume pairing.

	E [MeV]			$B(EL, 0 \to L)$ $\left[e^2 \text{ fm}^{2L}\right]$		
Phonons	Exp.	Surface	Volume	Exp.	Surface	Volume
2^+	1.171	1.941	1.497	2.016×10^3	1.766×10^3	1.364×10^3
3^-	—	3.313	2.500	—	1.396×10^5	1.380×10^5
4^+	—	3.757	2.478	—	1.568×10^6	4.518×10^5

In Fig. 1, the Gamow–Teller strength distribution in ^{120}Sn is calculated in the QRPA model and in the QRPA+QPVC model respectively. The results using volume pairing and surface pairing force are compared. At the QRPA level, the GT strength distributions in the low-energy region obtained by using volume and surface pairing force are similar. In the giant resonance region, the basic feature is the same where three peaks are present, however, for the volume pairing case, the strength of the third peak is the highest, while for the surface pairing case, the middle peak has the highest transition strength. Going from QRPA to QRPA+QPVC, a large spreading width of about 4.5 MeV is developed for either pairing force, and the difference between the results obtained from two types of pairing force becomes smaller. In the GTR region $E = 13$–25 MeV, the centroid energies obtained in QRPA with the volume and the surface pairing force are 16.97 and 17.00 MeV

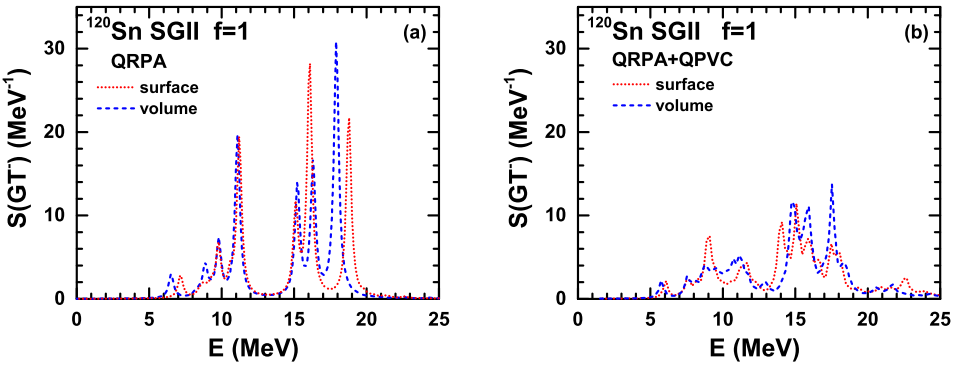

Fig. 1. Gamow–Teller strength distribution in ^{120}Sn calculated in the QRPA [panel (a)] and in the QRPA+QPVC [panel (b)] model with volume and surface pairing, using the Skyrme interaction SGII.

respectively, while they become 16.87 and 16.89 MeV in QRPA+QPVC. The stability of the centroid found going from QRPA to QRPA+QPVC is related to the use of the subtraction method in the present calculation.

In Fig. 2, the Gamow–Teller strength distributions obtained with surface pairing and volume pairing are compared with experimental data. We use a smearing parameter $\Delta = 0.5$ MeV in the QRPA and QRPA+QPVC calculation, instead of the value $\Delta = 0.2$ previously used in Fig. 1. This value corresponds to the energy resolution of the (p, n) experiment [44]. The cross section from (p, n) reaction is normalized by the unit cross section to give the strength distribution shown in Fig. 2 [28]. Going from QRPA to QRPA+QPVC, a much larger width is developed for both pairing forces, leading to a much better agreement with experimental data. However, the agreement with data is not as good as that calculated with the interaction SkM* [28].

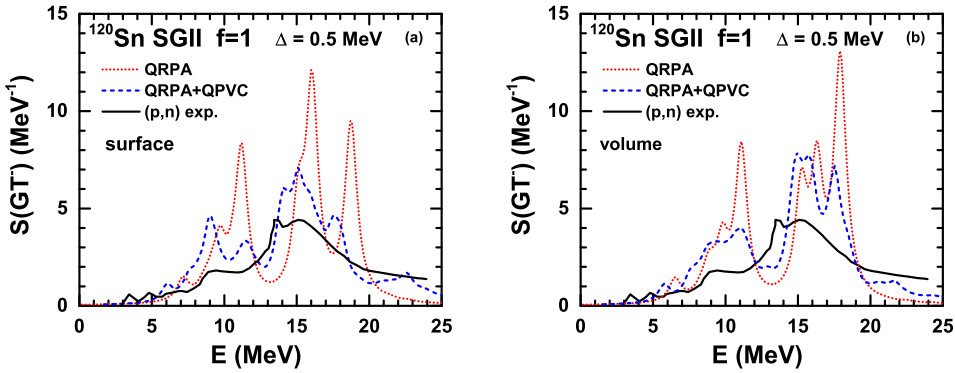

Fig. 2. Gamow–Teller strength distribution in ^{120}Sn calculated by QRPA and QRPA+QPVC model with surface [panel (a)] and volume [panel (b)] pairing, using Skyrme interaction SGII. The smearing parameter $\Delta = 0.5$ MeV is used instead of $\Delta = 0.2$ MeV used for Fig. 1. The experimental data [44] from (p, n) reaction are shown for comparison.

4. Summary

The GT excitation of ^{120}Sn is studied by the self-consistent QRPA+QPVC model based on the Skyrme density functional SGII. Two different zero-range pairing forces, of volume- and surface-type, are employed in the calculations, and the resulting phonon properties and the GT strength distribution obtained with either force are compared. It turns out that the overall properties of the GT strength distribution calculated by QRPA+QPVC model with these two types of pairing forces are similar, although there are some differences in the details of the fragmentation process. With the inclu-

sion of QPVC effect, a large spreading width is developed, and the agreement of the theoretical GT strength distribution with the experimental data is improved.

REFERENCES

[1] H.-Th. Janka *et al.*, *Phys. Rep.* **442**, 38 (2007).
[2] K. Langanke, G. Martínez-Pinedo, *Rev. Mod. Phys.* **75**, 819 (2003).
[3] Z.M. Niu, *Phys. Lett. B* **723**, 172 (2013).
[4] Y.F. Niu, N. Paar, D. Vretenar, J. Meng, *Phys. Rev. C* **83**, 045807 (2011).
[5] N. Paar, G. Colò, E. Khan, D. Vretenar, *Phys. Rev. C* **80**, 055801 (2009).
[6] H.Z. Liang, Y.F. Niu, N. Van Giai, J. Meng, *J. Phys.: Conf. Ser.* **267**, 012042 (2011).
[7] N. Paar, D. Vretenar, T. Marketin, P. Ring, *Phys. Rev. C* **77**, 024608 (2008).
[8] E. Caurier *et al.*, *Rev. Mod. Phys.* **77**, 427 (2005).
[9] S.E. Koonin, D.J. Dean, K. Langanke, *Phys. Rep.* **278**, 1 (1997).
[10] C.L. Bai *et al.*, *Phys. Rev. C* **90**, 054335 (2014).
[11] M. Bender, J. Dobaczewski, J. Engel, W. Nazarewicz, *Phys. Rev. C* **65**, 054322 (2002).
[12] S. Fracasso, G. Colò, *Phys. Rev. C* **72**, 064310 (2005).
[13] S. Fracasso, G. Colò, *Phys. Rev. C* **76**, 044307 (2007).
[14] J. Li, G. Colò, J. Meng, *Phys. Rev. C* **78**, 064304 (2008).
[15] P. Sarriguren, *Phys. Rev. C* **91**, 044304 (2015).
[16] K. Yoshida, N. Van Giai, *Phys. Rev. C* **78**, 064316 (2008).
[17] Z.M. Niu *et al.*, *Phys. Rev. C* **95**, 044301 (2017).
[18] N. Paar, T. Nikšić, D. Vretenar, P. Ring, *Phys. Rev. C* **69**, 054303 (2004).
[19] N. Paar, D. Vretenar, E. Khan, G. Colò, *Rep. Prog. Phys.* **70**, 691 (2007).
[20] G.F. Bertsch, P.F. Bortignon, R.A. Broglia, *Rev. Mod. Phys.* **55**, 287 (1983).
[21] P.F. Bortignon, R.A. Broglia, D.R. Bes, R. Liotta, *Phys. Rep.* **30**, 305 (1977).
[22] G. Colò, N. Van Giai, P.F. Bortignon, R.A. Broglia, *Phys. Rev. C* **50**, 1496 (1994).
[23] E. Litvinova *et al.*, *Phys. Lett. B* **730**, 307 (2014).
[24] T. Marketin, E. Litvinova, D. Vretenar, P. Ring, *Phys. Lett. B* **706**, 477 (2012).
[25] Y.F. Niu *et al.*, *Phys. Rev. C* **85**, 034314 (2012).
[26] Y.F. Niu, G. Colò, E. Vigezzi, *Phys. Rev. C* **90**, 054328 (2014).
[27] Y.F. Niu, Z.M. Niu, G. Colò, E. Vigezzi, *Phys. Rev. Lett.* **114**, 142501 (2015).
[28] Y.F. Niu *et al.*, *Phys. Rev. C* **94**, 064328 (2016).

[29] C. Robin, E. Litvinova, *Eur. Phys. J. A* **52**, 205 (2016).
[30] C.L. Bai *et al.*, *Phys. Lett. B* **719**, 116 (2013).
[31] J. Engel *et al.*, *Phys. Rev. C* **60**, 014302 (1999).
[32] Y. Fujita *et al.*, *Phys. Rev. Lett.* **112**, 112502 (2014).
[33] Z.M. Niu *et al.*, *Phys. Rev. C* **87**, 051303 (2013).
[34] Z.Y. Wang, Y.F. Niu, Z.M. Niu, J.Y. Guo, *J. Phys. G: Nucl. Part. Phys.* **43**, 045108 (2016).
[35] H. Sagawa, C.L. Bai, G. Colò, *Phys. Scr.* **91**, 083011 (2016).
[36] P. Ring, P. Schuck, *The Nuclear Many-Body Problem*, Springer-Varlag, Berlin, Heidelberg 1980.
[37] D. Gambacurta, M. Grasso, J. Engel, *Phys. Rev. C* **92**, 034303 (2015).
[38] K. Moghrabi, M. Grasso, G. Colò, N. Van Giai, *Phys. Rev. Lett.* **105**, 262501 (2010).
[39] X. Roca-Maza, Y.F. Niu, G. Colò, P.F. Bortignon, *J. Phys. G: Nucl. Part. Phys.* **44**, 044001 (2017).
[40] V.I. Tselyaev, *Phys. Rev. C* **75**, 024306 (2007).
[41] V.I. Tselyaev, *Phys. Rev. C* **88**, 054301 (2013).
[42] N. Van Giai, H. Sagawa, *Phys. Lett. B* **106**, 379 (1981).
[43] `http://www.nndc.bnl.gov`
[44] M. Sasano *et al.*, *Phys. Rev. C* **79**, 024602 (2009).